A Fixed-Frequency DSOGI-PLL Technique for Robust Phase and Frequency Detection in Weak Grids

Sumant Kumar *1, Anjana Tripathi2, Balram Yadav3

- * M.Tech Student, School of Electrical & Electronics Engineering, Scope global skills university, Bhopal, M.P. ssumantbhp@gmail.com 1
- ²Assistant professor, School of Electrical & Electronics Engineering, Scope global skills university, Bhopal, M.P.

 anjana.tripathi2210@gmail.com²
 - ³HOD, School of Electrical & Electronics Engineering, Scope global skills university, Bhopal, M.P.

balram@sgsuniversity.ac.in3

ABSTRACT

The fixed-frequency DSOGI-PLL (FFDSOGI-PLL) is a new technique that eliminates estimation error under a variety of unbalanced grid conditions. The operating principle of FFDSOGI-PLL is introduced after the regular FADSOGI-PLL. Next, the stability performance of the system under several weak grid situations, including sag, swell, and harmonics, is evaluated between the FFDSOGI-PLL and the FADSOGI-PLL. Lastly, simulation results are shown to illustrate FFDSOGI-PLL's efficacy. One way to solve this it is essential to recalculate the errors at the off-nominal frequency and adjust the tuning frequency to a fixed value that corresponds to the nominal frequency. This provides a fast and stable approach for calculating the phase angle error and frequency error of the grid voltage with improved damping of its inherent harmonics, based on a fixed-frequency DSOGI-PLL known as FFDSOGI-PLL.

Keywords: - Three-phase PLL, FADSOGI, FFDSOGI, complex grid condition.

1. INTODUCTION

The resilience of renewable energy systems strengthens grid infrastructure, reduces the vulnerability of communities to power outages, and promotes energy access, particularly in remote or underserved areas. From a public health perspective, the transition to renewables brings tangible benefits, as it reduces air pollution and its associated health impacts, leading to improved well-being and quality of life for communities worldwide. Finally, on a global scale, the rapid deployment of renewable energy is indispensable for meeting climate targets and safeguarding the planet for future generations. In essence, the integration of renewable sources is not only desirable but imperative for navigating the complex challenges of the modern era. The assessment of the grid's phase and frequency becomes a crucial component for the integration of various energy sources. Within this thesis, the detection of Phase and Frequency as grid parameters is analyzed based on the FFDSOGI PLL model and the error in phase and frequency is obtained.

2. FREQUENCY FIXED DSOGI(FFDSOGI) PLL

By using a fixed frequency ω_0 , the frequency-fixed technique aims to alter the tuning frequency ω . Any Phase error that occurs due to fixed frequency is further compensated by the mathematical analysis. The final model is displayed in Fig. 1

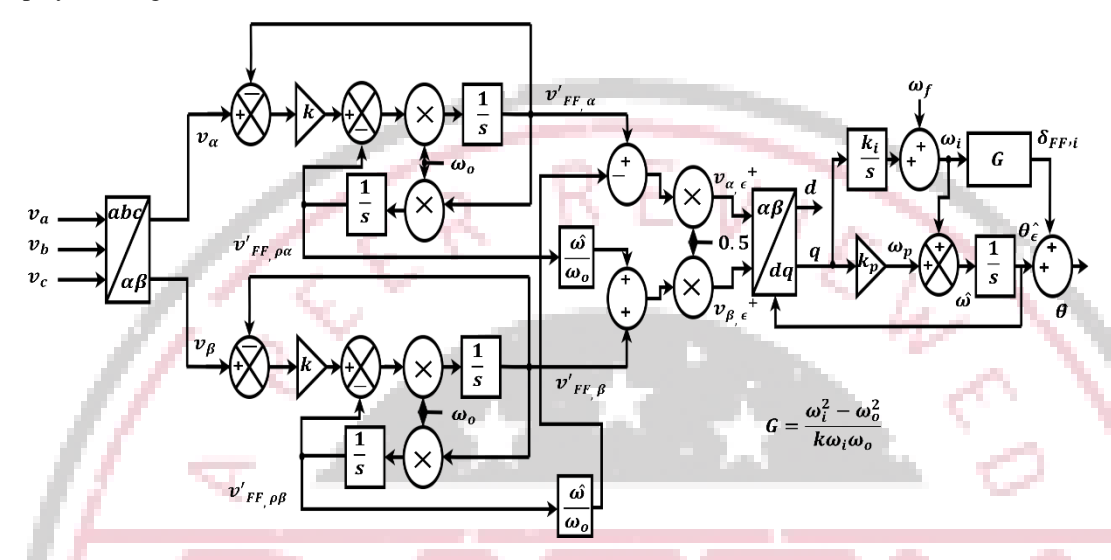


Fig. 1. Basic diagram of Three-Phase FFDSOGI PLL

3. MATHEMATICAL BEHAVIOUR ANALYSIS OF FFDSOGIPLL

To examine the behavior of FFDSOGI, both the SOGI are excited by eq. 1.1. and eq. 1.2. respectively.

Let

$$V_{\alpha}(t)=V_{\alpha}\cos(\omega t)$$
 (1.1)

$$V \beta (t) = V \beta \cos(\omega t)$$
 (1.2)

Apply the Laplace transform of equations (4.1.) and (4.2.) and then use Laplace Inverse to obtain, respectively, equations (1.3.) and (1.4.) to equations (1.5.) and (1.6.).

$$v_{FF,\alpha}'(t) = V_{\alpha} \left(\frac{k\omega_{o}\omega}{\sqrt{k^{2}\omega_{o}^{2}\omega^{2} + (\omega_{o}^{2} - \omega^{2})^{2}}} sin(\omega t - \delta_{FF}) - A sin(\sqrt{1 - \left(\frac{k}{2}\right)} 2\omega_{o}t - \emptyset_{1}) e^{-\frac{k\omega_{o}t}{2}} \right)$$
(1.3)

$$v_{FF,\rho\alpha}'(t) = V_{\alpha} \left(\frac{-k\omega_{o}^{2}}{\sqrt{k^{2}\omega_{o}^{2}\omega^{2} + (\omega_{o}^{2} - \omega^{2})^{2}}} \cos(\omega t - \delta_{FF}) + A\cos\left(\sqrt{1 - \left(\frac{k}{2}\right)} 2\omega_{o}t - \emptyset_{2}\right) e^{-\frac{k\omega_{o}t}{2}} \right)$$
(1.4)

$$v_{FF,\beta}'(t) = V_{\beta} \left(\frac{-k\omega_{o}\omega}{\sqrt{k^{2}\omega_{o}^{2}\omega^{2} + (\omega_{o}^{2} - \omega^{2})_{2}}} cos(\omega t - \delta_{FF}) + A \frac{\omega_{o}}{\omega} cos\left(\sqrt{1 - \left(\frac{k}{2}\right)} 2\omega_{o}t - \emptyset_{3}\right) e^{-\frac{k\omega_{o}t}{2}} \right)$$
(1.5)

$$v'_{FF,\rho\beta}(t) = V_{\beta} \left(\frac{-k\omega_{o}^{2}}{\sqrt{k^{2}\omega_{o}^{2}\omega^{2} + (\omega_{o}^{2} - \omega^{2})^{2}}} sin(\omega t - \delta_{FF}) + A \frac{\omega_{o}}{\omega} cos\left(\sqrt{1 - \left(\frac{k}{2}\right)} 2\omega_{o}t - \emptyset_{1}\right) e^{-k\omega_{o}t/2} \right)$$
(1.6)

Where,

$$A = \frac{k\omega\omega_o}{\sqrt{k^2\omega_o^2\omega^2 + (\omega_o^2 - \omega^2)2}\sqrt{1 - \left(\frac{k}{2}\right)^2}}$$

$$tan(\emptyset_1) = \frac{-\sqrt{(4-k^2)}(\omega_0^2 - \omega^2)}{k(\omega_0^2 + \omega^2)}$$

$$tan(\emptyset_3) = \frac{(k^2\omega^2 + 2\omega_o^2 - 2\omega^2)}{k\omega_o^2\sqrt{1 - \left(\frac{k}{2}\right)2}}$$

$$tan(\emptyset_{2}) = \frac{(k^{2}\omega_{o}^{2} - 2\omega_{o}^{2} + 2\omega^{2})}{2k\widehat{\omega}^{2}\sqrt{1 - \left(\frac{k}{2}\right)^{2}}}$$

$$sin(\delta) = \frac{\left(\omega^2 - \omega_o^2\right)}{\sqrt{k^2 \omega_o^2 \omega^2 + \left(\omega_o^2 - \omega^2\right)^2}}$$

On comparing (1.3.) with eq. (1.4.) to eq. (1.5.) with the eq. (1.6.), it is found that their in a steady state their magnitudes are not equal. If ω deviates from the fixed frequency ω_o , $V'_{FF,\alpha} = \frac{\omega_o}{\omega} V'_{FF,\rho\alpha}$ and $V'_{FF,\rho\beta} = \frac{\omega_o}{\omega} V'_{FF,\rho\beta}$. If a frequency difference occurs along with grid's unbalances, different positive sequence calculator (PSC) magnitude and hence ripple of second-order ripple come into existence in the SRF PLL output. To overcome this issue magnitude modification is done by multiplying the both in-phase and phase-quadrature signals with $\frac{\hat{\omega}}{\omega_o}$.

The Positive Sequence component's magnitude is accurate at the nominal frequency. However, there is a magnitude inaccuracy in the positive sequence component at off-nominal frequency. Therefore, it is necessary to adjust the phase-quadrature and in-phase signals in order to lessen the magnitude mistake that arises at the off-nominal frequency. Calculations based on nominal frequency assume a stable power system. However, deviations from this frequency can introduce errors or complications in calculations, particularly in positive sequence analysis, which is crucial for understanding the behaviour of balanced three-phase systems.

4. EXTRACTION OF POSITIVE SEQUENCE COMPONENT WITH FFDSOGI

As per the required magnitude adjustment and applying the eq (1.3) to (1.6), the output signal of the positive signal calculator is:

$$\begin{bmatrix} v_{\alpha,\in}^+(t) \\ v_{\beta,\in}^+(t) \end{bmatrix} = \frac{1}{2} \begin{bmatrix} v_{FF,\alpha}'(t) & -v_{FF,\rho\beta}'(t) \\ v_{FF,\beta}'(t) & v_{FF,\rho\alpha}'(t) \end{bmatrix} \begin{bmatrix} \frac{1}{\underline{\omega}} \\ \underline{\omega} \end{bmatrix}$$
(1.7)

Assuming $\widehat{\omega} = \omega + \Delta \omega$, eq (10) can be written as:

Research Journal of Engineering Technology and Medical Sciences (ISSN: 2582-6212), Volume 08, Issue 02, June-2025 Available at www.rjetm.in/

$$v_{\alpha,\in}^{+}(t) = K_{FF} \left[\frac{V_{\alpha} + V_{\beta}}{2} sin(\omega t - \delta_{FF}) + V_{\beta} \frac{\Delta \omega}{\omega} sin(\omega t - \delta_{FF}) \tau_{\alpha}(t) e^{-\frac{k\omega_{o}t}{2}} \right]$$
(1.8)

$$v_{\beta,\epsilon}^{+}(t) = K_{FF} \left[\frac{V_{\alpha} + V_{\beta}}{2} cos(\omega t - \delta_{FF}) + V_{\alpha} \frac{\Delta \omega}{\omega} cos(\omega t - \delta_{FF}) \tau_{\beta}(t) e^{-\frac{k\omega_{o}t}{2}} \right]$$
(1.9)

Where.

$$K_{FF} = \frac{k\omega_0 \omega}{\sqrt{k^2 \omega_0^2 \omega^2 + (\omega_0^2 - \omega^2)^2}} \tag{1.10}$$

Due to the insignificance of the need for the exact terms of the oscillating component of the signal and decaying terms of the signal, both are concise as $\tau_{\alpha}(t)$ and $\tau_{\beta}(t)$ and declines to zero exponentially with a rate having time-constant of $\tau_{p} = \frac{2}{k\omega_{0}}$.

In summary, if the system's input frequency ω differs from ω_0 , there exists a phase shift δ_{FF} . This conclusion can be drawn from equations (1.7) and (1.8). Furthermore, two terms with a dependency of $\Delta\omega/2\omega$ will arise if the estimated frequency $\hat{\omega}$ by the FFDSOGI is not equal to ω , causing an imbalance in the system.

Moreover, (1.9) shows the magnitudes of both expressions (1.7) and (1.8), which depend on the system's frequency difference. In the event that the amplitude needs to be recalculated, (1.10) can be roughly

$$K_{FF} \cong \frac{2(\omega - \omega_0)^2}{k^2 \omega_0^2} + 1$$

For minor ω variations from ω_0 . Figure 1. shows the error of this approximation.

5. ANALYSIS OF FFDSOGI PLL

Utilizing the transformation of Clarke and Park with an alignment of α to q axis, (1.8) and (1.9) with $\widehat{\theta_{\epsilon}} = \widehat{\omega}t - \delta_{FF}$ and $\theta_{FF} = \omega t - \delta_{FF}$ respectively, The components d and q are ascertained as follows:

$$v_d(t) = V \cos(\theta_{FF} - \hat{\theta}_{\epsilon}) + D_{d \cdot \Delta \omega}(t) + \tau_d(t) e^{-\frac{k\omega_0 t}{2}}$$
(1.11)

$$v_q(t) = V \sin(\theta_{FF} - \hat{\theta}_{\epsilon}) + D_{q,\Delta\omega}(t) + \tau_q(t)e^{-\frac{k\omega_0 t}{2}}$$
(1.12)

Where,

$$V = K_{FF} \frac{V_{\alpha} + V_{\beta}}{2}$$

$$D_{d'\Delta\omega}(t) = K_{FF} \frac{\Delta\omega}{2\omega} \left(\frac{V_{\alpha} + V_{\beta}}{2} \cos(\omega t - \widehat{\omega}t) + \frac{V_{\alpha} - V_{\beta}}{2} \cos(\omega t + \widehat{\omega}t - 2\delta_{FF}) \right)$$

$$D_{q,\Delta\omega}(t) = K_{FF} \frac{\Delta\omega}{2\omega} \left(\frac{V_{\alpha} + V_{\beta}}{2} \sin(\omega t - \widehat{\omega}t) + \frac{V_{\alpha} - V_{\beta}}{2} \sin(\omega t + \widehat{\omega}t - 2\delta_{FF}) \right)$$

The magnitudes of the oscillating component and decaying component terms are concise as $\tau_d(t)$ and $\tau_q(t)$. Under locked conditions, $cos(\theta_{FF} - \hat{\theta}_{\epsilon}) \cong 1$ and $sin(\theta_{FF} - \hat{\theta}_{\epsilon}) \cong (\theta_{FF} - \hat{\theta}_{\epsilon})$ respectively, for which $v_d(t)$ yields the magnitude and $v_d(t)$ gives the system's phase error information.

To examine positive sequence harmonics of h order eq. (1.13) and (1.14) is applied to eq. (1.13) to (1.12) and dq component is obtained in eq. (1.15) and (1.16) and shows oscillation will occur of h-1 order.

$$V_{\alpha}(t) = V_h \sin(h\omega t + \emptyset_h) \tag{1.13}$$

$$V_{\beta}(t) = -V_h \cos(h\omega t + \emptyset_h) \tag{1.14}$$

$$D_{d,h}(t) = V_h \frac{h+1}{2} |v_{FF,\rho h}| \cos((h-1)\omega t + \varphi_h)$$
(1.15)

$$D_{q,h}(t) = V_h \frac{h+1}{2} |v_{FF,\rho h}| \sin((h-1)\omega t + \varphi_h)$$
(1.16)

6. EXPERIMENTAL PARAMETERS

The Proposed model is taken into consideration for the following three test scenarios:

- a 10% and 80% Voltage Sag
- a 10% and 80% Voltage Swell
- a harmonic injection 20% of the 3RD Harmonic and 50% of the 5TH Harmonic

The parameters considered for FFDSOGI and FADSOGI PLL are:

Table I. Parameter for Phase Frequency error estimation in FFDSOGI and FADSOGI

MODEL	FFDSOGI	FADSOGI
k	$\sqrt{2}$	$\sqrt{2}$
ω_n	$2\pi 16.877$	$2\pi 16.877$
k_p	$2\zeta\omega_n$	$2\zeta\omega_n$
k_i	ω_n^2	ω_n^2
W_f	$2\pi 16.877$	÷ /
ζ	1	1
	$\overline{\sqrt{2}}$	$\overline{\sqrt{2}}$

6.1 UNBALANCE VOLTAGE SAG

i) 10% Sag

A Sag of 10% is created in phase A at time t=0.4 sec and then voltage is restored at time t=0.8 sec in grid voltage. The system's estimated frequency and phase are observed in MATLAB SIMULINK MODEL for the case of FFDSOGI PLL and FADSOGI PLL in fig. (2).

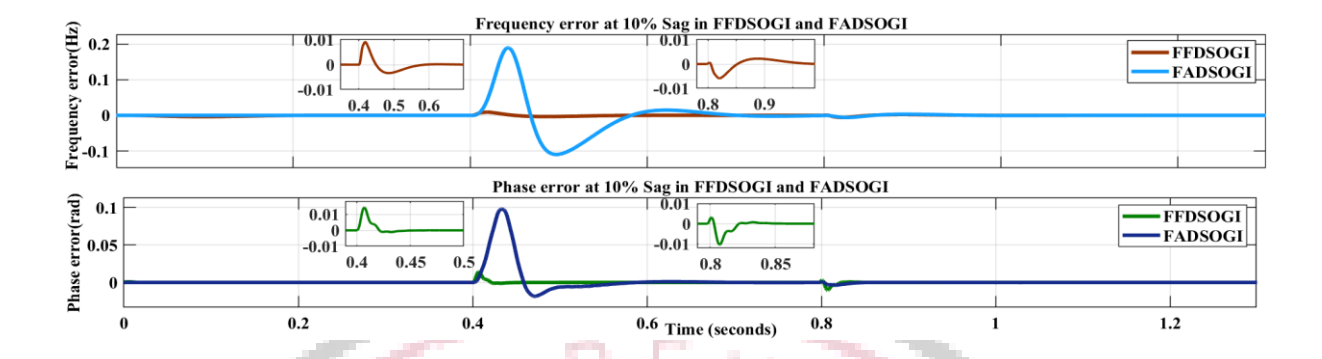


Fig. 2. Frequency and Phase error at 10% SAG in FFDSOGI and FADSOGI PLL

ii) 80% Sag

A Sag of 80% is created in phase A at time t=0.4 sec and then voltage is restored at time t=0.8 sec in grid voltage. The system's estimated frequency and phase are observed in MATLAB SIMULINK MODEL for the case of FFDSOGI PLL and FADSOGI PLL In Fig. (3).

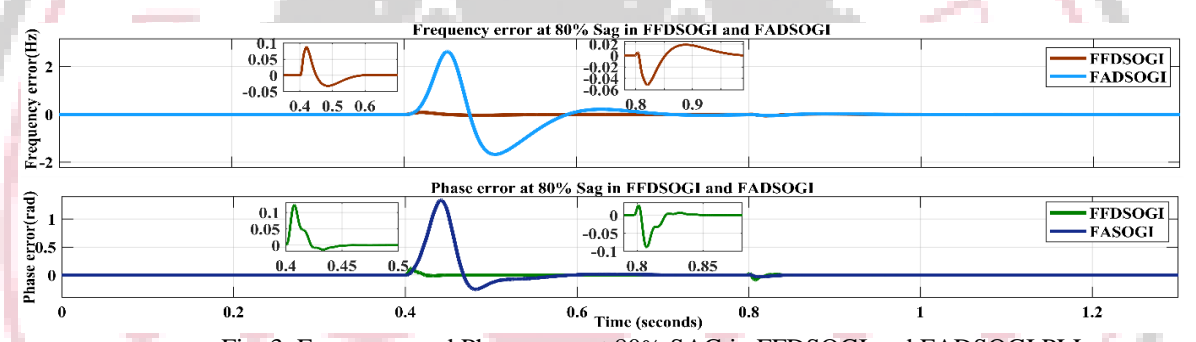


Fig. 3. Frequency and Phase error at 80% SAG in FFDSOGI and FADSOGI PLL

6.2 UNBALANCE VOLTAGE SWELL

i) 10% Swell

A Swell of 10% is created in phase A at time t=0.4 sec and then voltage is restored at time t=0.8 sec in grid voltage. The system's estimated frequency and phase are observed in MATLAB SIMULINK MODEL for the case of FFDSOGI PLL and FADSOGI PLL in fig.(4)

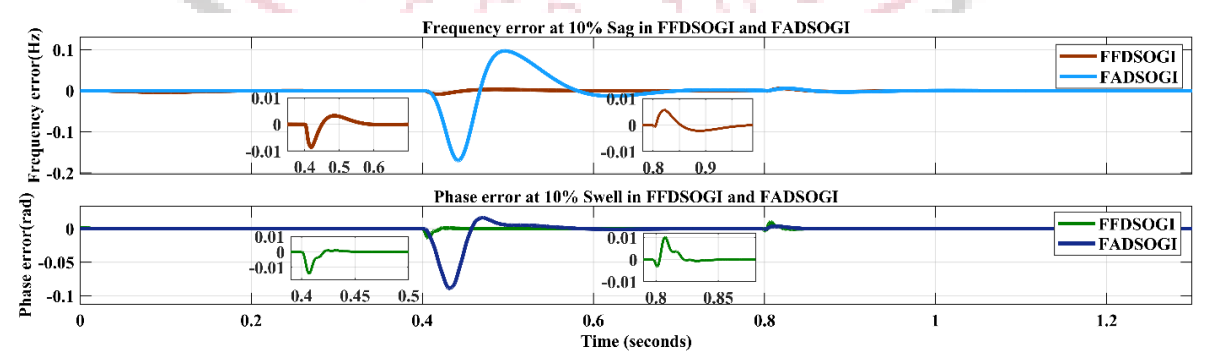


Fig. 4. Frequency and Phase error at 10% SWELL in FFDSOGI and FADSOGI PLL

ii) 80% Swell

A Swell of 80% is created in phase A at time t=0.4 sec and then voltage is restored at time t=0.8 sec in grid voltage. The system's estimated frequency and phase are observed in MATLAB SIMULINK MODEL for the case of FFDSOGI PLL and FADSOGI PLL in Fig. (5).

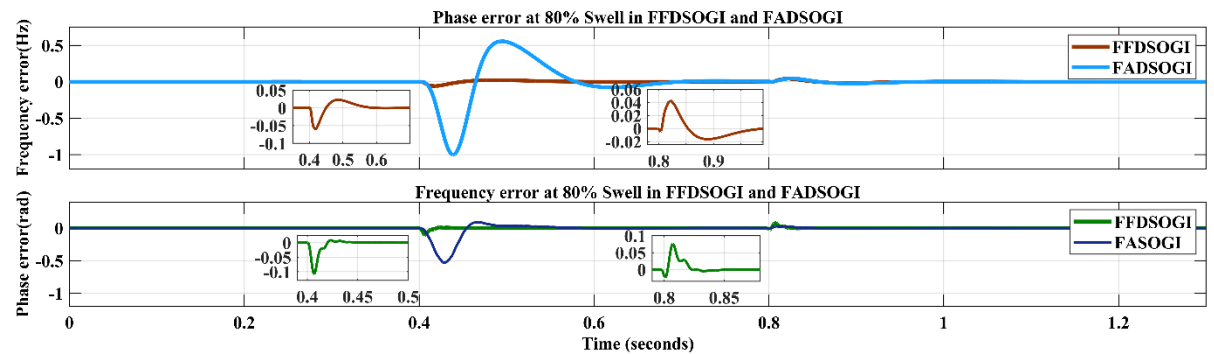


Fig. 5. Frequency and Phase error at 80% SWELL in FFDSOGI and FADSOGI PLL

7. ERROR IN QUANTIZED FORM

Table II. Peak error in Frequency estimation in FFDSOGI and FADSOGI

	Peak Error in Frequency Estimation in Hz					
Sl No.	Grid Condition	FFDSOGI		FADSOGI		
	-	Max.	Min.	Max.	Min.	
1	10% Sag	0.008971	-0.00562	0.1889	-0.10860	
2	80% Sag	0.086741	-0.051405	2.6311	-1.6723	
3	10% Swell	0.005776	-0.00850	0.09682	-0.1697	
4	80% Swell	0.042683	-0.055904	0.5526	-1.0035	
5	5 th Harmonics	0.0011	-0.0011	0.0010	0.0010	
6	3 rd Harmonics	0.0038	-0.0037	0.0022	-0.0019	

Table III. Peak error in Phase estimation in FFDSOGI and FADSOGI

Peak Error in Phase Estimation in radians					
Sl No.	Grid Condition	FFDSOGI		FADSOGI	
		Max.	Min.	Max.	Min.
1	10% Sag	0.01352	-0.010108	0.097946	-0.018543
2	80% Sag	0.12251	-0.085560	1.32	-0.26
3	10% Swell	0.010209	-0.013656	0.01639	-0.08715
4	80% Swell	0.076113	-0.1078	0.085472	-0.1078
5	5 th Har.	0.0211	-0.0218	0.00512	0.0051
6	3 rd Har.	0.0347	-0.0347	0.00806	-0.0082

Table IV. Settling time in Frequency error in sec.

Sl. No	Sag/Swell	FFDSOGI	FADSOGI
1	10%	0.18	0.28
2	80%	0.17	0.27

Table V. Settling time in Phase error in sec.

Sl. No	Sag/Swell	FFDSOGI	FADSOGI
1	10%	.03	0.13
2	80%	0.02	0.12

7.1 COMPLEXITY REPORT OF MODEL



Fig. 6. Complexity Report of FFDSOGI PLL

Complexity Report of FADSOGI PLL

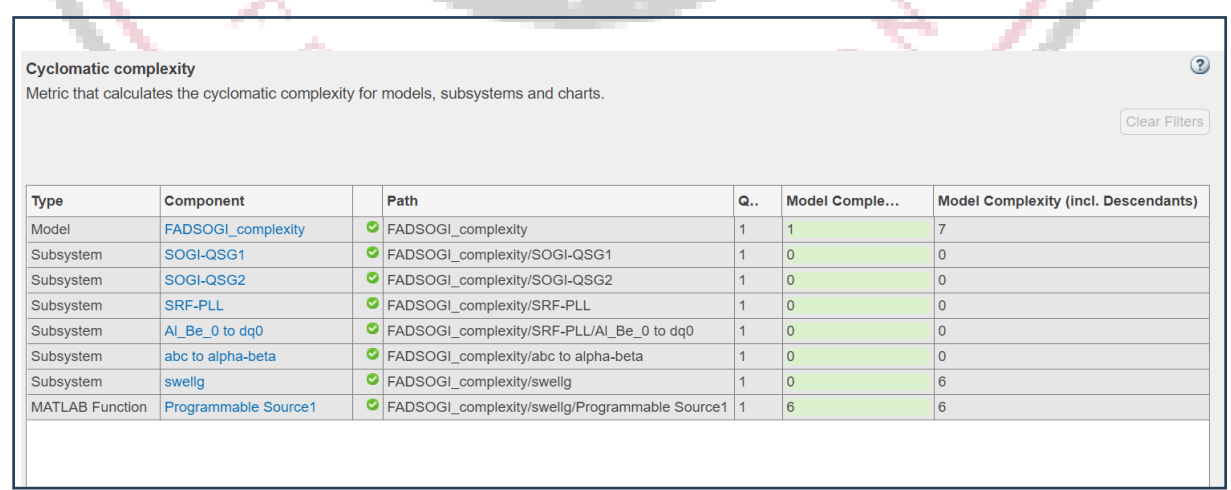


Fig. 7. Complexity Report of FADSOGI PLL

8. CONCLUSION

As can be seen from the experimental result for the Sag of 10% and sag of 80% in both cases FFDSOGI Performed better in terms of error amplitude. The same is the case of Swell, for the Swell of 10% and sag of 80% in both cases, FFDSOGI performed better. For the case of 50% of the 5th Harmonics and 20% of the 3rd harmonics, FFDSOGI gives more error in phase and frequency compared to FADSOGI. In comparison to the frequency and phase error settling time of FADSOGI PLL, the FFDSOGI PLL has a shorter settling time.

By the complexity analysis of the model FFDSOGI model comes to be less complex compared to the FADSOGI. Hence overall FFDSOGI performed better.

REFERENCES

- [1] Li et al., "Robust Frequency-Adaptive Second-Order Generalized Integrator PLL for Single-Phase Grid-Tied Applications," *IEEE Trans. on Industrial Electronics*, 2022.
- [2] Morales et al., "A Double Second-Order Generalized Integrator-Based Phase-Locked Loop for Grid-Connected Power Converters Under Distorted Grid Conditions," *IEEE Trans. on Industrial Electronics*, 2017.
- [3] Han et al., "Robust Double Second-Order Generalized Integrator PLL for Three-Phase Grid-Connected Converters Under Grid Voltage Disturbances," *IEEE Trans. on Power Electronics*, 2019.
- Wang et al., "Adaptive Double-Second-Order Generalized Integrator PLL for Three-Phase Grid-Tied Converters Under Dynamic Grid Conditions," *IEEE Trans. on Power Electronics*.
- Liu et al, "Enhanced Double-Second-Order Generalized Integrator PLL with Harmonic Compensation for Three-Phase Grid-Connected Converters," IEEE Trans. on Industrial Electronics, 2022.
- [6] L. Hadjidemetriou, E. Kyriakides, Y. Yang, and F. Blaabjerg, "A synchronization method for single-phase grid-tied inverters," *IEEE Trans. Power Electron.*, vol. 31, pp. 2139-2149, March 2016.
- [7] M. Karimi-Ghartemani and M. R. Iravani, "A method for synchronization of power electronic converters in polluted and variable-frequency environments," *IEEE Trans. Power Syst.*, vol. 19, no. 3, pp. 1263-1270, August 2004.
- [8] "A Critical Examination of Frequency-Fixed Second-Order Generalized Integrator-Based Phase-Locked Loops," *IEEE Trans. Power Electron.*, vol. 32, no. 9, September 2017.
- [9] Benjamin Hoepfner and Ralf Vick, "Symmetrical Components Detection With FFDSOGI-PLL Under Distorted Grid Conditions," *IEEE Trans.*, 2019.
- [10] Benjamin Hoepfner and Ralf Vick, "A Three-Phase Frequency-Fixed DSOGI-PLL with Low Computational Effort," *IEEE Acess*, April 2023.

